Article:
Li, Liangjun, Yue, Hangbo, Wu, Qiqi et al. (4 more authors) (2022) Unveiling the reinforcement effects in cottonseed protein/polycaprolactone blend biocomposites. Composites science and technology. 109480. ISSN: 0266-3538

https://doi.org/10.1016/j.compscitech.2022.109480

Journal Pre-proof

Unveiling the reinforcement effects in cottonseed protein/polycaprolactone blend biocomposites

Liangjun Li, Hangbo Yue, Qiqi Wu, Juan P. Fernández-Blázquez, Peter S. Shuttleworth, James H. Clark, Jianwei Guo

PII: S0266-3538(22)00222-6

DOI: https://doi.org/10.1016/j.compscitech.2022.109480

Reference: CSTE 109480

To appear in: *Composites Science and Technology*

Received Date: 31 December 2021

Revised Date: 15 April 2022

Accepted Date: 20 April 2022

Please cite this article as: Li L, Yue H, Wu Q, Fernández-Blázquez JP, Shuttleworth PS, Clark JH, Guo J, Unveiling the reinforcement effects in cottonseed protein/polycaprolactone blend biocomposites, *Composites Science and Technology* (2022), doi: https://doi.org/10.1016/j.compscitech.2022.109480.

CRediT author statement

Liangjun Li: Investigation; Data curation; Software; Formal analysis; Writing - original draft.

Hangbo Yue: Conceptualization; Supervision; Formal analysis; Funding Acquisition; Writing - original draft, review & editing.

Qiqi Wu: Methodology; Investigation.

Juan P. Fernández-Blázquez: Formal analysis; Writing - review & editing.

Peter S. Shuttleworth: Methodology; Writing - review & editing.

James H. Clark: Supervision; Writing review & editing.

Jianwei Guo: Conceptualization; Supervision; Writing - review & editing.

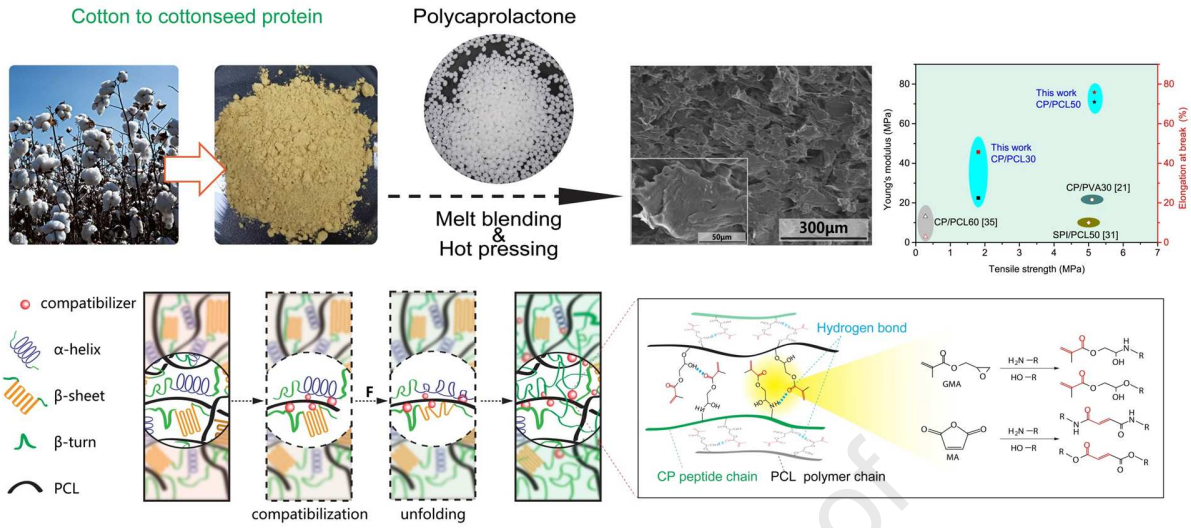

Unveiling the reinforcement effects in cottonseed protein/polycaprolactone blend biocomposites [1]

Liangjun Li [a], Hangbo Yue [a, b] *, Qiqi Wu [a,] Juan P. Fernández-Blázquez [c], Peter S. Shuttleworth [d], James H. Clark [e], and Jianwei Guo [a, *]

[a] *School of Chemical Engineering and Light Industry, Guangdong University of Technology, Guangzhou 510006, China*

[b] *Guangdong Provincial Key Laboratory of Plant Resources Biorefinery, Guangdong University of Technology, Guangzhou 510006, China*

[c] *IMDEA Materials Institute, Getafe, 28906 Madrid, Spain*

[d] *Department of Polymer Physics, Elastomers and Energy, Institute of Polymer Science and Technology, CSIC, 28006 Madrid, Spain.*

[e] *Green Chemistry Centre of Excellence, University of York, York YO10 5DD, UK*

Abstract: Cottonseed protein (CP) was compounded with polycaprolactone (PCL) in different concentrations by melt blending, and then hot-pressed to prepare CP/PCL blend films. A co-continuous phase is formed when the CP/PCL content is 50/50, and the tensile strength, modulus and toughness are 9, 10, and 63 times greater than that of neat CP film. This remarkable improvement is mainly due to the intrinsic flexibility of long PCL polymer chains, whilst the polymeric crystalline structure can still be formed. Furthermore, 1wt% of compatibilizing agent — glycidyl methacrylate (GMA) or maleic anhydride (MA), is added to the blends. Measurements from scanning electron microscopy (SEM), X-ray photoelectron spectroscopy (XPS) and Fourier transform

[1] *Corresponding author: Tel.: +86 20 39322232. E-mail: hangbo.yue@gdut.edu.cn (H.Y), guojw@gdut.edu.cn (J.G).

infrared spectroscopy (FTIR) showed the presence of chemically reactive compatibilization between the compatibilizer and CP or PCL phase, and the two phases with strong binding forces are well dispersed. Meanwhile, the compatibilizer can induce the protein secondary structure to unfold, further increasing the physical compatibilization between the protein and polymer chains, which has a noticeable contribution to the blend's mechanical, hydrophobic properties and thermal stability. This work adds new element to the knowledge of compatibilization in terms of optimised interfaces of polymer blends, and provide new insights into fabricating high performance protein derived bioplastics and biocomposites.

Keywords: Bio composites (A); Interphase (B); Mechanical properties (B); compatibilization; plant protein

1. Introduction

The non-degradability of traditional petroleum-based polymeric plastics, especially microplastics[1], poses a threat to the environment and even human health[2]. One of the key solutions is to develop environmentally friendly bioplastics that are fully degradable. Within this area there are two main research hotspots. One is the use of biodegradable aliphatic polyesters, such as polylactic acid[3], poly(butylene succinate)[4], and poly (butyleneadipate-co-terephthalate)[5]. The other is naturally biodegradable polymers. In particular, low cost by-products of the food/agriculture industry provide rich protein sources, such as rapeseed oil protein[6], crayfish shell protein[7], chicken feather keratin[8], cottonseed protein[9]. Cottonseed protein (CP) is a high-quality plant protein with a globulin content of 90% that after hydrolysis contains 18 amino acids similar to soybean protein[10]. In addition, the global output of cottonseed from 2019 to 2020 was 44.95 million tons demonstrating its largescale availability[11]. Currently it is mainly used as animal feed source[12], or goes to waste.

There are a number of successful examples using protein to prepare higher

value-added bioplastics and composites. In particular, considering the inferior mechanical properties of protein-based bioplastics, efforts in cross-linking[9] and natural fibre reinforcement[13] have sought to rectify to some degree these deficiencies. Also, blending the protein with biodegradable synthetic polymers has been shown to be an effective strategy. For example, the addition of polyurethane prepolymer (PUP) improved the toughness of its blend soy protein composites, though the wet tensile strength was slightly slower[14]. In another example, CP was blended with poly(vinyl alcohol) PVA and then solution-casted to prepare CP/PVA blend films[15]. At higher CP concentrations there were visible signs of agglomeration, indicating the limited compatibility between the CP and PVA. Several plasticizers that can form hydrogen bonds with both species were used. Interestingly, feather keratin and PVA can experience macromolecular chain entanglements after blending, which improves the mechanical properties of feather keratin/PVA electro-spun nanofibers[8].

Polycaprolactone (PCL) has been widely used in applications of degradable plastics[16], porous nanomaterials[17], hot melt adhesive[18], and biomedical materials[19]; due to its excellent biodegradability, biocompatibility, high flexibility, and processibility[20]. Additionally, there have been a number of reports on the improvement in the properties of protein polymers, by blending PCL with them. For instance, with incrementing PCL blend content above 5wt%, the maximum stress and Young's modulus of rapeseed protein/PCL biocomposites increased[6]. In the case of blending crayfish protein with 30wt% PCL the maximum strain fracture was improved by approximately 38%[7]. Similar PCL reinforcement effects were also found in soy protein/PCL[21] and wheat gluten/PCL[22] blend biocomposites. Nevertheless, hydrophobic PCL are incompatible to hydrophilic bio-derived polymers; methods of plasma treatment[23], and addition of nano-hydroxyapatite[24] in scaffold polymers were reported to address this issue. Successful application of small-molecule

compatibilizers (e.g., coconut oil[25], methylenediphenyl diisocyanate MDI[26], MA [27]) have been shown to improve the interfacial compatibility in these types of protein/biopolyester blends.

However, these compatibilizers can react only with the protein and not with the hydrophobic polymer, limiting the degree of compatibility between the components. Modifying the PCL with a small amount (2.5wt%) of anhydride improved the tensile strength 2-3 times in the wheat gluten/PCL blends, which were thought to be due to both improved chemical and physical interactions, and consequently better dispersions of the gluten phase within the continuous PCL phase[28]. In addition, PUP was found to improve the compatibility of soy protein-polyesters composite through chemical bonding[29]. The isocyanate groups(N=C=O) of PUP can react with the soy protein functional groups via urethane linkages to enhance the interaction between them. However, to synthesize PUP, PCL glycol and toxic MDI need to be reacted under vacuum, and stirred continuously at high speed and temperature.

Glycidyl methacrylate (GMA) and MA consisting of active functional groups (e.g., vinyl, epoxy, and anhydride) have been widely used for interface improvement in plastic/rubber blends, and being considered herein as reactive compatibilizer. More importantly, how to effectively achieve compatibilization in degradable protein/polymer blends, especially revealing possible physical/chemical interactions between the components (e.g., transformation of protein secondary structure) in this biocomposite system still remains unclear. In this study, PCL was melt-blended with CP and then hot-pressed to produce CP/PCL blend biocomposite films. The effects of PCL content on the morphology and properties of the biocomposites were investigated. Results showed that the interfacial compatibility of the CP/PCL blends was improved by adding a small amount of GMA or MA molecules, which resulted in a uniform CP dispersion and formation of a continuous PCL phase. These materials showed significant

improvement in tensile strength, modulus, toughness, and thermal stability. The strengthening mechanism involving interfacial chemical compatibilization and physical synergistic compatibilization induced by protein structure transformation is explained and proved through systematic differential scanning calorimetry (DSC), X-Ray diffraction (XRD), FTIR and XPS characterization.

2. Material and methods

Materials. CP powder (protein content about 50% measured by the Kjeldahl method) was obtained from Qingdao Kerui Culture Medium, China. Polycaprolactone was purchased from Perstorp UK (CAPA®6500) with a relative molecular weight of 50000, and a OH value of ca.2 mg KOH/g. Urea, sodium hydroxide, glycerol and anhydrous ethanol were purchased from Tianjin Damao chemical reagent factory. Compatibilizers GMA and MA were provided by Shanghai Maclean biochemical technology. Dicumyl peroxide (DCP) was provided by Shanghai Aladdin Biochemical Technology. All reagents were analytically pure and used as received without further purification.

CP pre-treatment. The procedures used to denature and plasticise CP were reported previously[9]. Briefly, CP and urea were mixed in water and kept stirring for 4 hours at room temperature, and the pH of the mixture adjusted to pH 11 using 1 mol L^{-1} NaOH before being heated to 70 ºC for 30 min. Then, glycerol was added and the mixture stirred for another 30 min before being heated in an oven at 80 ºC for 48 hours. At this stage the pre-dried material was crushed into granules, and then heated at 80 ºC again for 48 h until a constant weight was achieved.

Melt Blending. CP granules, PCL, and compatibilizer were melt-blended in a torque rheometer (XSS, Shanghai Kechuang Rubber Machinery Equipment) at 30 rpm for 20 min. The rheometer chamber temperature was set at 130 ºC. A tiny amount of an initiator, DCP (5%, relative to the compatibilizer weight) generating free radicals at high temperature in a short time, was added for better formation of entangled polymer chains

networks during the blend compounding process[4, 30]. Sample nomenclatures are: CP/PCL0, CP/PCL10, CP/PCL30, CP/PCL50, CP/PCL100, where the number represents the mass fraction of PCL in the blend. CP/PCL30/GMA1 and CP/PCL30/MA1 represent the sample CP/PCL30 containing 1wt% GMA or MA.

Hot Pressing. After melt-blend compounding, a certain amount of the product was placed between stainless steel plates (width = 700 mm, length = 700 mm, thickness = 0.75) covered with aluminium foil. It was then transferred to the hot-press (HY-25TS, Shanghai Hengyu Instrument) for 5 min at 120 ℃, 20 MPa. Afterwards, the obtained CP/PCL samples were stored under vacuum for 24 h before use.

Details in instrumental characterization and a schematic illustration of the fabrication procedures can be found in Supporting information.

3. Results and Discussion

3.1. CP/PCL blend compounding

Bioplastic composites were prepared by melt compounding CP with different amounts of reinforcing component PCL, followed by hot-press moulding, as illustrated in Fig. S1. Flexible polymer films/sheets with the desired thickness were obtained. Cross-section images in Fig. 1a-b show granules in CP/PCL0 and CP/PCL10, formed as protein agglomerates[9, 13], leading to a rough and uneven surface (Fig. 1f-g). This protein agglomeration has been found in some protein-polymer blends, and usually presents a droplet-like morphology[29]. Generally, hydrophobic PCL with terminated hydroxyl group functionality is incompatible with more hydrophilic proteins consisting of carboxyl and amine groups at chain ends. Phase separation between CP and PCL occurs at low PCL concentrations. The protein is only weakly aggregated and as such, is partially separated revealing a flaky structure as in the case for the sample CP/PCL30 (Fig. 1c). This scaly feature is very similar to the strong ductile fracture morphology in other polymer biocomposites[31]. Furthermore, a co-continuous phase is formed when

the CP/PCL mixing content is equivalent (CP/PCL50). The scaly morphology in this specimen is even more evident (Fig. 1d), and similar to that of CP/PCL100 (Fig. 1j), indicating that the addition of PCL can increase the plastic flowability of the blend films, which is consistent with the tensile test results (Fig. 2 and Table 1). Additionally, well-distributing cavities appeared after chloroform etching treatment, as shown in Fig. 1 k-n. Both number and size of these cavities increase when higher amount of PCL was present in the biocomposites, indicating well dispersion of PCL phase within CP matrix.

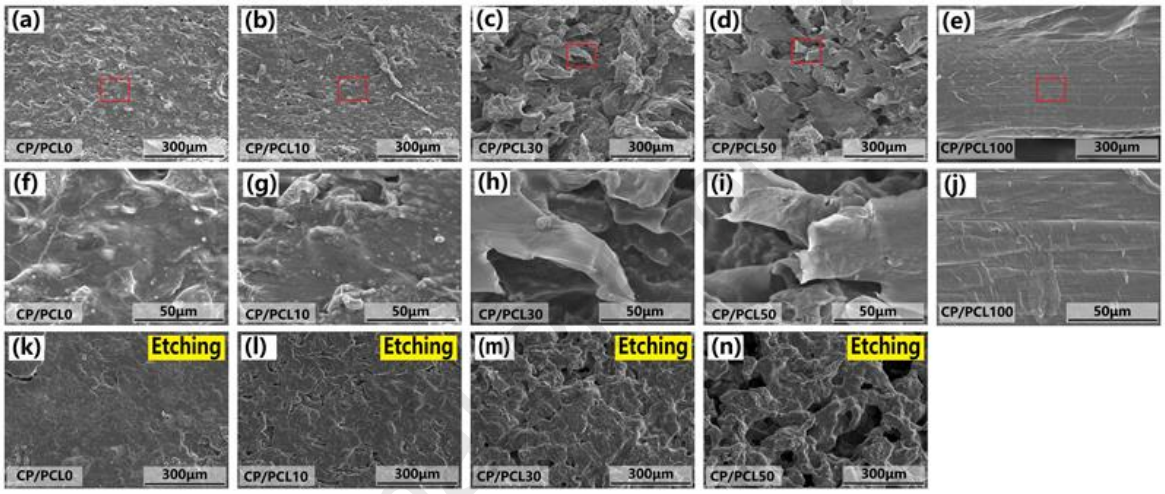

Fig. 1.

The effects of blending PCL content on mechanical properties of CP/PCL blend films were investigated by standard tensile testing, with typical stress-strain curves shown in Fig. S2. While mechanical strength of neat CP and CP/PCL10 are very low (< 1 MPa), strength and toughness of the CP/PCL blends significantly improved as the PCL content increased. For example, the tensile strength, Young's modulus, and toughness of CP/PCL50 are 5.1 MPa, 71 MPa, and 328 kJ/m^3, respectively, which are 9, 10 and 60 times greater than that of the neat CP film. For CP/PCL30, the strength, modulus, and elongation at break were improved by 3 times compared to CP/PCL0. Interestingly, this strength increase only appears when a threshold amount of PCL is reached. For CP/PCL10 sample, the presence of phase separation (Fig. 1b, g) deteriorates stress transfer, and the binding forces between components are close to the weakest. Similar

threshold of modulus increase has been found in rapeseed meal/PCL blend at 5wt% PCL[6], and in soy protein/montmorillonite (MMT) at 1.6wt% MMT[32]. Moreover, the CP/PCL blends display good mechanical properties comparable to other protein/polymer blends, as seen in Table 1. Compared to the literature reference of the same composite component blend, CP/PCL60[18], the tensile strength and Young's modulus of our CP/PCL50 was 18 and 5.4 times stronger, respectively (Table 1). Moreover, the elongation at break of CP/PCL30 in this study is 4 times higher than that of CP/PVA30 (70wt% CP and 30wt% polyvinyl alcohol)[15], and two times greater than SPI/PCL50[29]. The increase in elongation at break is even more evident for our CP/PCL50 sample, mainly due to the ductility contribution of PCL. These results suggest that the use of PCL as a reinforcing phase for protein blend composites is attractive, especially when it comes to ductility enhancement.

Table 1. Mechanical properties of CP/PCL blend samples. Six other similar protein/polymer blend biocomposites are included for comparison.

Samples	Tensile strength (MPa)	Young's modulus (MPa)	Elongation at break (%)	Toughness (kJ m^{-3})	Ref.
CP/PCL0	0.58±0.07	7.40±0.98	13.72±1.52	5.22±0.45	
CP/PCL10	0.37±0.07	4.94±0.71	11.22±1.94	2.67±0.88	
CP/PCL30	1.81±0.17	22.50±4.35	45.66±5.18	64.98±8.85	
CP/PCL50	5.17±0.48	70.96±8.73	75.83±14.86	328.5±92.2	this
CP/PCL100	20.79±1.84	110.5±4.07	947.9±87.5	/	work
CP/PCL30/GMA1	2.67±0.16	41.30±2.33	50.87±2.27	117.9±7.07	
CP/PCL30/MA1	1.96±0.30	33.92±2.92	45.3±8.75	75.18±26.82	
CP Concentrate	2.55±0.25	16.53±1.88	62.2±13.3	/	[13]

CP40/PCL60	0.28±0.06	13.1±3.83	2.9±0.4	/	[28]
CP/PVA30	6.0	/	10.0	/	[15]
SPI/PCL50	5.1	/	4.60	/	[32]
Crayfish/PCL30	2.0	110	40.0	~800	[10]
Rapeseed/PCL20	0.32	0.32	8.0	/	[34]

It was speculated that the PCL addition on the improvement of the tensile strength and modulus is strongly related to the formation of PCL crystalline structures. To verify this, DSC and XRD experiments were carried out. Fig. 2a shows DSC heating and subsequent cooling curves of the CP/PCL blends. The endothermic peak that appeared in the heating stage at a T_m of approximately 51 ºC is the melting peak of semi-crystalline PCL. Clearly, the area of this melting peak increases with increasing PCL content. The appearance of a shoulder peak for the CP/PCL10 and CP/PCL30 is due to melting of smaller PCL crystals. During the cooling stage, neat PCL crystallizes at T_c around 20 ºC while CP/PCL50 and CP/PCL10 at 15 ºC and 10 ºC, respectively. This decrease in T_c is ascribed to kinetically unfavourable PCL crystallization in the presence of nearby abundant CP biomacromolecules, which is commonly seen in semi-crystalline polymer blends like PCL/PLA[33]. The presence of the CP phase leads to the formation of a less ordered PCL crystalline structure, with lower T_m and degree of crystallinity (X_c%) relative to the neat PCL. Detailed DSC thermal results are listed in Table S1, with the obtained X_c% results showing the same tendency as those obtained from XRD, decreasing with higher CP content (see Fig. S3).

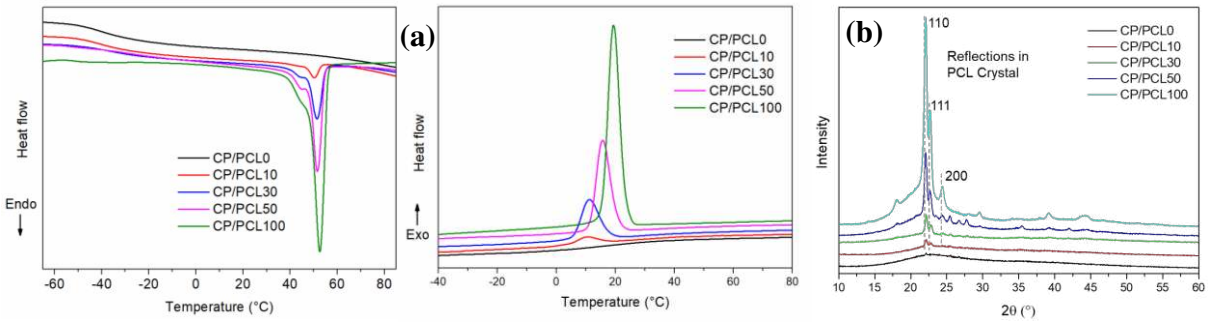

Fig. 2.

In Fig. 2b, all samples showed three clear diffraction peaks at the same position, corresponding to (110), (111), and (200) planes of PCL crystals, which indicates that the presence of amorphous CP has a negligible impact on the PCL crystalline structure. Nevertheless, the reduced intensity of the three diffraction peaks suggests that the CP chains hinder the formation of PCL crystallites. Moreover, the long period interlamellar distance might be affected, as co-continuous phase (Fig. 1d) presented in CP/PCL blends is likely to generate microphase-separation influence on the confined crystallization of PCL[34, 35]. Further study on this scenario is under investigation using small angle X-ray scattering.

To understand better the interactions occurring between the CP/PCL blend components and if they are of a chemical or physical nature, FTIR spectra were recorded (see Fig. 3a). The absorption peak at 2953 cm^{-1} corresponding to the methylene C-H stretching vibration grows in intensity with increasing PCL content. A similar tendency was found for the peaks at 1726 cm^{-1}, which is ascribed to the stretching vibrations of the carbonyl (C=O) group. The stretching vibrations of the ether group (C-O-C) display two characteristic peaks at 1255 cm^{-1} and 1163 cm^{-1}. The amide I (stretching vibration of C=O in peptide chains) at 1621 cm^{-1}, amide II (N-H in-plane bending [36]) that usually occurs at 1500~1600 cm^{-1}, and amide III bands (C=O bending and C-N stretching vibrations[9]) at 1455 cm^{-1} can all be identified. Apart from change in peak intensity relating directly to increased PCL content, there are no new

discernible peaks nor peak shifts that is consistent with only physical interactions occur between CP and PCL polymer chains.

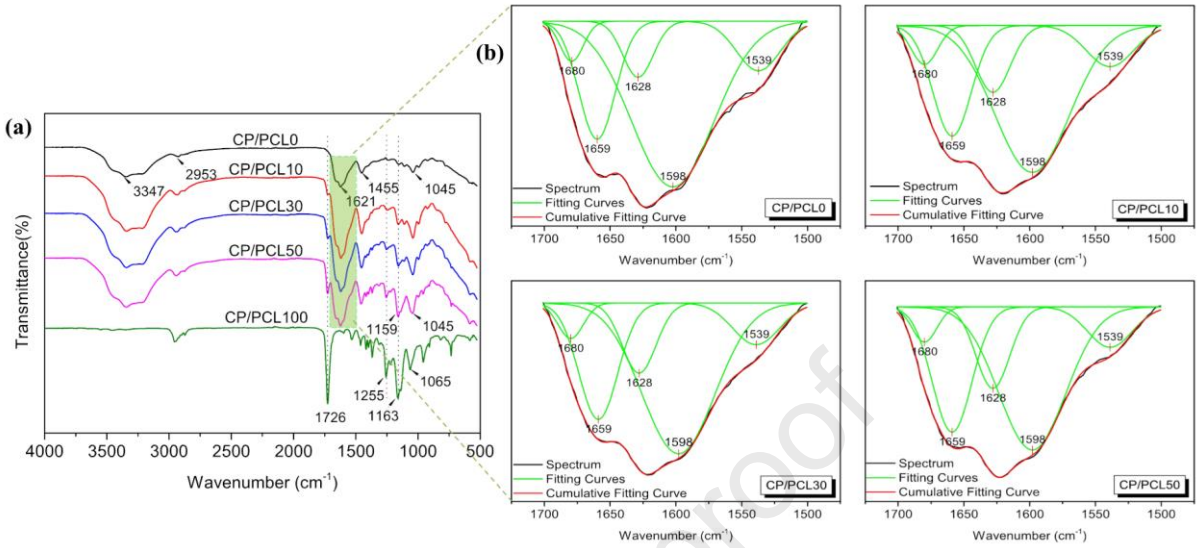

Fig. 3.

Interestingly, information about secondary structure of protein (like regularly ordered α-helix and β-sheet forms, and the irregular β-turn form) can be obtained by analysing infrared spectra through peak deconvolution of protein amide band[37, 38]. Successful examples on revealing the changes of secondary structure using this method were found in black turtle beanan lectin[39] and food proteins[40]. Detailed spectral analysis and the estimated percentage of the protein secondary structure are shown in Fig.3b, and Table S2, respectively. From the estimated percentages, the α-helix and β-sheet are the predominant forms increasing from a total of 85% for the neat protein (CP/PCL0) to nearly 90% as the PCL content in the blends increases, with a subsequent drop in the β-turn percentage. That means the PCL blending treatment is likely to promote the ordered transformation of protein secondary structure. However, hydrogen bonding within the structure would be strengthened, reducing possible CP/PCL chain entanglements. To overcome this, a compatibilizer was applied to weaken the hydrogen bonding and create possible chemical interactions between the CP and PCL components.

3.2. Improvement of CP/PCL interfacial compatibility

Further CP/PCL30 films were prepared by adding 1% GMA or MA compatibilizer. It was found from tensile testing results (Table 1) that the addition of a small amount of either compatibilizing agent had a noticeable improvement on the mechanical properties compared to the CP/PCL30 films without the GMA or MA. For instance, the Young's modulus of CP/PCL30/GMA1 doubled from 22.5 MPa (CP/PCL30) to 41.3 MPa, and that of CP/PCL30/MA1 increased 1.5 times to 33.9 MPa. Furthermore, the tensile strength and toughness of CP/PCL30/GMA1 showed a 47% and 100% improvement. The compatibilization effect can also be observed from their microscopic morphology. In Fig. 4, the scaly-like continuous phase can again be observed indicating that it has a ductile morphology. For the compatibilized samples (CP/PCL30/GMA1 and CP/PCL30/MA1), this ductile morphology is more apparent, in line with their higher values of elongation and toughness (Table 1). After etching treatment, the ductile morphology disappeared (Fig. 4g-i); instead, cavities uniformly distributed in CP/PCL30/GMA1 and CP/PCL30/MA1, in contrast to CP/PCL30, suggesting good phase dispersion in the compatibilized samples. From closer inspection of Fig. 4d, tiny protein particles are still present in the CP/PCL30 sample. However, the size of these particles is significantly reduced after adding GMA or MA (marked by arrows in Fig. 4e and Fig. 4f), indicating less phase separation within the biocomposite. Therefore, interfacial compatibility between CP and PCL chains could be improved by adding a small amount of the chosen compatibilizer. These results were further confirmed by identifying the pixel distribution and estimation of the grayscale / colour gamut using optical microscopy (see Fig. S4 and Table S3).

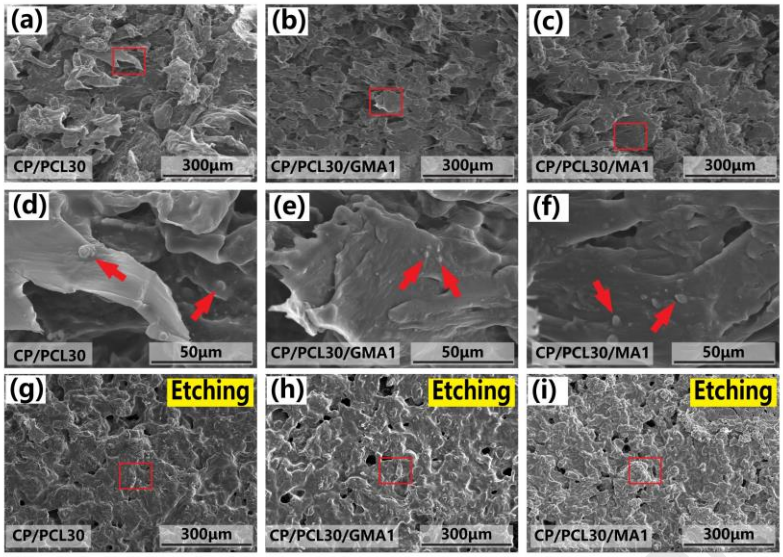

Fig. 4.

The improved CP/PCL compatibility slightly reduces the crystallinity of PCL (Table S1). However, it seems to have had less impact on their thermal performance, with TGA and DTG curves (Fig. S5) being very similar to the non-compatibilized sample CP/PCL30. Thermal degradation kinetic experiments were conducted by heating samples at four different rates (5, 10, 20 and 25 ºC min^{-1}). The apparent activation energy E_a was then calculated using the differential Kissinger method [44], as shown in Equation (1)

$$\ln\left(\frac{\beta}{T_p^2}\right) = \ln\left(\frac{AR}{Ea}\right) - \frac{Ea}{RT_p} \quad (1)$$

where β is the heating rate (K s^{-1}), A the frequency factor (s^{-1}), R the ideal gas constant (8.314 J mol^{-1} K^{-1}), T_p the maximum decomposition temperature (K). The activation energy E_a of the thermal decomposition process can be obtained from the slope of the plot ln ($\beta/(T_p^2)$ vs. $1/T_p$. It was found (Table 2) that E_a of the CP/PCL biocomposites containing GMA or MA was noticeably higher than that of the control sample CP/PCL30. For instance, after adding 1wt% MA, E_a is increased by 19%, suggesting that more energy is required to initiate decomposition. In other words, the compatibilized samples enjoy stronger binding forces and higher thermal stability than that without treatment.

Table 2. Thermal decomposition temperature and activation energy of CP/PCL samples.

Samples	$T_{10\%}$ (°C)	T_{CP} (°C)	T_{PCL} (°C)	E_a (kJ/mol)	Residual (%)
CP/PCL30	185	235	399	208	15.9
CP/PCL30/GMA1	195	238	398	235	14.1
CP/PCL30/MA1	187	237	402	246	15.6

Note: $T_{10\%}$, T_{CP} and T_{PCL} corresponds to the temperature at 10% weight loss, the maximum CP and PCL weight loss, respectively.

Furthermore, the hygroscopicity (equilibrium moisture absorption) decreased by 16.57% and water diffusion coefficient decreased by about 30% when 1wt% of GMA was added to CP/PCL30, see results in Table S4. The improvement of hydrophobicity is mainly due to the formation of more tightly bounded interfaces induced by the compatibilizer. A dense network structure of CP/PCL30/GMA1 (higher density vs. CP/PCL30, Table S4) would make water molecules much difficult to diffuse in materials[41].

3.3. Reinforcement Mechanism

In addition to the protein secondary structure transformation and enhanced hydrogen bonding described previously, further insights into chemically reactive compatibilization between the compatibilizer and the CP or PCL were analysed using FTIR and XPS. In Fig. 5a, compared to CP/PCL30, the peak intensity at 1726 cm^{-1} (C=O stretching vibration) and 1159 cm^{-1} (C-O-C asymmetric vibration) in CP/PCL30/GMA1 and CP/PCL30/MA1 increased. Furthermore, the peak position of the amide I band shifted from 1620 cm^{-1} to 1624 cm^{-1} (Fig. 5b) after the addition of the compatibilizer GMA or MA; this shift is often ascribed to the changes in the protein secondary structure[42]. More importantly, new peaks at 1593 cm^{-1} and 1594 cm^{-1} appeared in CP/PCL30/GMA1 and CP/PCL30/MA1, respectively, indicating chemical

reactions have taken place during the compatibilization treatment. Possible chemical reactions between the compatibilizer (GMA or MA), protein and PCL are illustrated in Fig. 5c. Glycidyl methacrylate and maleic anhydride have epoxy and anhydride groups at chain ends, being able to react with hydroxyl or amino groups [43] and form the new functional group -C(=O)-C=C-. As such, the newly developed peaks at 1593 cm^{-1} and 1594 cm^{-1} are likely due to the stretching vibration of the double bonds in unsaturated alkene substituted by carbonyl group, whose absorption often appears near 1600 cm^{-1} [44]. A tentative reinforcing mechanism in the CP/PCL blend biocomposite is proposed in Fig. 5d. For blend compounding PCL with CP, polymer chain entanglements and hydrogen bonding are the main driving forces to enhance CP/PCL interactions. When the small molecules GMA or MA are present in the same system, on the one hand, they can migrate and penetrate into the CP/PCL interfaces, contributing to CP chain-unfolding and transformation of the protein secondary structure from α-helix and β-sheet to β-turn. This phenomenon is similar to the compatibilizing action of clay and MMT nanofillers in polymer blend composites [45, 46]. Nevertheless, the migration and penetration process would be affected by a number of factors like molecular size, viscosity, and surface free energy[47, 48]. The increased amount of disordered β-turn structure (Table S2) is expected to aid mechanical properties of the protein derived biocomposites [15]. On the other hand, hydrogen bonding within the system would be weakened during the protein unfolding transformation, thus exposing a greater proportion of reactive -NH_2 and -OH functional groups. As a consequence, there will be more chance for the chemically reactive compatibilization effect to occur (Fig. 5c), further enhancing the CP/PCL interfacial bonding strength. Quantitative analysis of the interfacial thickness of polymer blends would be considered to provide detailed length scale information[49].

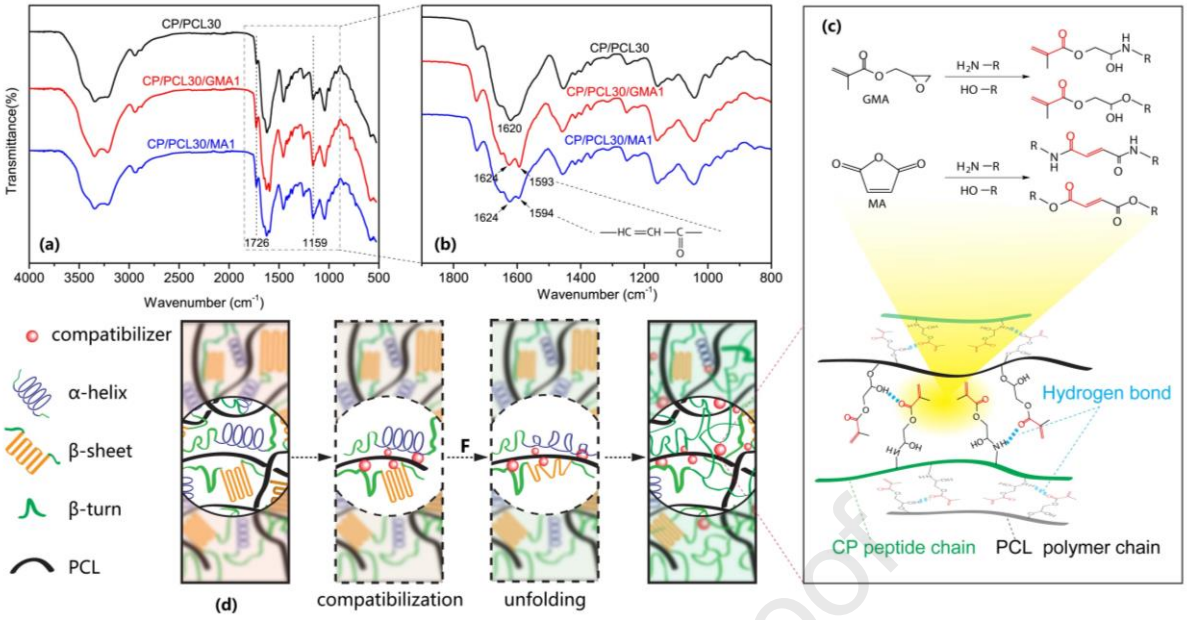

Fig. 5.

Additional evidence is provided by XPS. Results of element analysis in Table S4 indicate that the nitrogen content in CP/PCL30/GMA1 and CP/PCL30/MA1 has increased, which has to originate from the cottonseed protein amino groups as GMA and MA contain no nitrogen. Specifically, nitrogen increment is most likely due to the exposure of the -NH_2 group after compatibilization treatment and unfolding of the ordered protein structure (Fig. 5d). A similar explanation is plausible for the additional oxygen content (Table S5) from increased exposure of the protein -OH groups.

Fig. 6 shows the C1s and O1s binding energies of the compatibilized samples CP/PCL30/GMA1 and CP/PCL30/MA1 compared to the control sample, CP/PCL30. Clearly, in the C1s spectrums with binding energy peaks at 284.8 eV (C-C bond), 286.3 eV (C-N or C-O bond), and the O1s spectrums at 531.3 eV related to the O-C bond remain unaltered. However, the binding energies associated with the C=O bonds in both C1s and O1s spectra increase by 0.1eV. In addition, from the FTIR of the compatibilized samples shown in Fig. 5 a-b, there is evidence of sp^2 C=C hybridised carbon, which typically gives rise to an electron-absorbing conjugation effect (nuclear potential V_n), and a reduced shielding effect (nucleus valence electron repulsion

potential V_v)[50]. Overall, the total C1s and O1s binding energies (the sum of V_n and V_v) of the C=O bond slightly increases. These characteristics in the XPS spectra further confirm the unsaturated bond formation due to the GMA/MA compatibilization treatment, and suggest the occurrence of chemically reactive compatibilization.

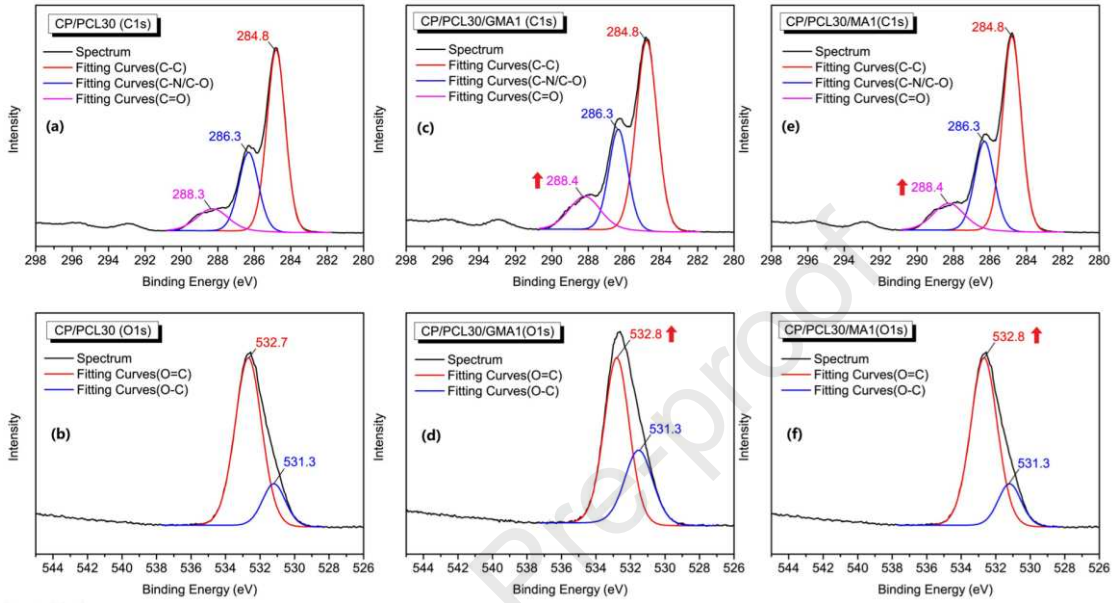

Fig. 6.

4. Conclusion

Biodegradable protein/polymer blend biocomposites with desirable mechanical and thermal properties were fabricated via compounding of cottonseed protein with polycaprolactone by melt blending and hot-pressing. This simple CP/PCL blend compounding mainly involves physical chain entanglement and hydrogen bonding between the two blend phases. Moreover, the excellent flexibility of the long PCL polymer chains and its crystalline structure contribute to improved mechanical properties whilst above the noted threshold concentration. The addition of 5% compatibilizer (e.g., glycidyl methacrylate) plays a significant role in the even dispersion of the blend phases, helping their interfacial compatibility. Specifically, the compatibilizer can induce the unfolding transformation of the protein secondary structure, from α-helix and β-sheet into the disordered β-turn structure, which brings

deeper understanding of molecular structure evolution during the process and adds new element to the knowledge of compatibilization of polymer blends[51]. A synergistic strengthening effect (physical compatibilization between protein and PCL polymer chains, and chemically reactive compatibilization at functional interfaces among the compatibilizer, CP and PCL macromolecules) presented in this work is likely to be applied to other protein/polymer blend biocomposites, providing insight into fabricating high performance protein derived bioplastics. Likely potential applications of this type of blend biocomposites include plywood adhesives[18], biomedical engineering[20], packing sheet, and agriculture flower/plant pot[13], etc. Measurements of biodegradability of the blend biocomposites using soil-burial tests are under investigation.

CRediT authorship contribution statement

Liangjun Li: Investigation; Data curation; Software; Formal analysis; Writing - original draft. Hangbo Yue: Conceptualization; Supervision; Formal analysis; Funding Acquisition; Writing - original draft, review & editing. Qiqi Wu: Methodology; Investigation. Juan P. Fernández-Blázquez: Formal analysis; Writing - review & editing. Peter S. Shuttleworth: Methodology; Writing - review & editing. James H. Clark: Supervision; Writing review & editing. Jianwei Guo: Conceptualization; Supervision; Writing - review & editing.

Declaration of competing interest

The authors declare that they have no known competing financial interests or personal relationships that could have appeared to influence the work reported in this paper.

Acknowledgements

This work was supported by National Natural Science Foundation of China (21706039), Natural Science Foundation of Guangdong Province (2022A1515011500), Guangdong Provincial Key Laboratory of Plant Resources Biorefinery

(2021B1212040011), and China Scholarship Council. P.S.S. gratefully acknowledges financial support from the Ministerio de Ciencia e Innovación for the PID2020-117573-GB-I00 grant.

References

[1] C.M. Rochman, Microplastics research—from sink to source, Science 360 (2018) 28-29.

[2] S. Rist, B.C. Almroth, N.B. Hartmann, T.M. Karlsson, A critical perspective on early communications concerning human health aspects of microplastics, Sci. Total. Environ. 626 (2018) 720-726.

[3] X.H. Zhao, K. Li, Y. Wang, H. Tekinalp, G. Larsen, D. Rasmussen, et al., High-strength polylactic acid (PLA) biocomposites reinforced by epoxy-modified pine fibers, ACS Sustain. Chem. Eng. 8 (2020) 13236-13247.

[4] F. Wu, M. Misra, A.K. Mohanty, Sustainable green composites from biodegradable plastics blend and natural fibre with balanced performance: Synergy of nano-structured blend and reactive extrusion, Compos. Sci. Technol. 200 (2020) 108369.

[5] S.J. Xiong, B. Pang, S.J. Zhou, M.K. Li, S. Yang, Y.Y. Wang, et al., Economically competitive biodegradable PBAT/Lignin composites: Effect of lignin methylation and compatibilizer, ACS Sustain. Chem. Eng. 8 (2020) 5338-5346.

[6] M. Delgado, M. Felix, C. Bengoechea, Development of bioplastic materials: From rapeseed oil industry by products to added-value biodegradable biocomposite materials, Ind. Crop. Prod. 125 (2018) 401-407.

[7] M. Felix, A. Romero, J.E. Martin-Alfonso, A. Guerrero, Development of crayfish protein-PCL biocomposite material processed by injection moulding, Compos. Part B-Eng. 78 (2015) 291-297.

[8] M. He, B.N. Zhang, Y. Dou, G.Q. Yin, Y.D. Cui, X.J. Chen, Fabrication and characterization of electrospun feather keratin/poly(vinyl alcohol) composite nanofibers,

RSC Advances 7 (2017) 9854-9861.

[9] H.B. Yue, Y.D. Cui, P.S. Shuttleworth, J.H. Clark, Preparation and characterisation of bioplastics made from cottonseed protein, Green Chem. 14 (2012) 2009-2016.

[10] C. Marquie, S. Guilbert. Formation and properties of cottonseed protein films and coatings. In: A Gennadios, editor. Protein-based films and coatings, Florida: CRC Press; 2002.

[11] World agricultural production, Circular Series WAP 07-20 July 2020, United States Department of Agriculture.

[12] J. Wang, G. Clark, M. Ju, S. Castillo, D.M. Gatlin, Effects of replacing menhaden fishmeal with cottonseed flour on growth performance, feed utilization and body composition of juvenile red drum Sciaenops ocellatus, Aquaculture 523 (2020) 735217.

[13] H.B. Yue, Y.R. Zheng, P.X. Zheng, J.W. Guo, J.P. Fernandez-Blazquez, J.H. Clark, et al., On the improvement of properties of bioplastic composites derived from wasted cottonseed protein by rational cross-linking and natural fiber reinforcement, Green Chem. 22 (2020) 8642-8655.

[14] Y. Chen, L. Zhang, L. Du, Structure and Properties of Composites Compression-Molded from Polyurethane Prepolymer and Various Soy Products, Ind. Eng. Chem. Res. 42 (2003) 6786-6794.

[15] W.J. Chen, J. Ding, X.M. Yan, W. Yan, M. He, G.Q. Yin, Plasticization of cottonseed protein/polyvinyl alcohol blend films, Polymers 11 (2019) 2096.

[16] J.H.M. Hernandez, Effect of the incorporation of polycaprolactone (PCL) on the retrogradation of binary blends with cassava thermoplastic starch (TPS), Polymers 13 (2020) 38.

[17] N.B. Tolou, H. Salimijazi, T. Dikonimos, G. Faggio, G. Messina, A. Tamburrano, et al., Fabrication of 3D monolithic graphene foam/polycaprolactone porous nanocomposites for bioapplications, J. Mater. Sci. 56 (2021) 5581–5594.

[18] H.N. Cheng, C.V. Ford, Z. He, Evaluation of polyblends of cottonseed protein and polycaprolactone plasticized by cottonseed oil, Int. J. Polym. Anal. Ch. 24 (2019) 389-398.

[19] E. Malikmammadov, T.E. Tanir, A. Kiziltay, V. Hasirci, N. Hasirci, PCL and PCL-based materials in biomedical applications, J. Biomat. Sci-Polym. E. 29 (2018) 863-893.

[20] R.A. Ilyas, M.Y.M. Zuhri, M.N.F. Norrrahim, M.S.M. Misenan, M.A. Jenol, S.A. Samsudin, et al., Natural Fiber-Reinforced Polycaprolactone Green and Hybrid Biocomposites for Various Advanced Applications, Polymers 14 (2022) 182.

[21] Z.K. Zhong, X.Z.S. Sun, Properties of soy protein isolate/polycaprolactone blends compatibilized by methylene diphenyl diisocyanate, Polymer 42 (2001) 6961-6969.

[22] V.L. Finkenstadt, A.A. Mohamed, G. Biresaw, J.L. Willett, Mechanical properties of green composites with polycaprolactone and wheat gluten, J. Appl. Polym. Sci. 110 (2008) 2218-2226.

[23] B. Joseph, N. Ninan, R.M. Visalakshan, C. Denoual, R. Bright, N. Kalarikkal, et al., Insights into the biomechanical properties of plasma treated 3D printed PCL scaffolds decorated with gold nanoparticles, Compos. Sci. Technol. 202 (2021) 108544.

[24] M. Momeni, K. Amini, A. Heidari, M. Khodaei, Evaluation the Properties of Polycaprolactone/Fluorapatite Nano-biocomposite, J. Bionic. Eng. 19 (2022) 179-187.

[25] S.I. Hong, W.Y. Choi, S.Y. Cho, S.H. Jung, B.Y. Shin, H.J. Park, Mechanical properties and biodegradability of poly-ε-caprolactone/soy protein isolate blends compatibilized by coconut oil, Polym. Degrad. Stabil. 94 (2009) 1876-1881.

[26] K.I. Ku Marsilla, C.J.R. Verbeek, Mechanical Properties of Thermoplastic Protein From Bloodmeal and Polyester Blends, Macromol. Mater. Eng. 299 (2014) 885-895.

[27] A. Sasmal, D. Sahoo, R. Nanda, P. Nayak, P.L. Nayak, J.K. Mishra, et al., Biodegradable nanocomposites from maleated polycaprolactone/soy protein isolate

blend with organoclay: Preparation, characterization, and properties, Polym. Composite. 30 (2009) 708-714.

[28] J. John, J. Tang, M. Bhattacharya, Processing of biodegradable blends of wheat gluten and modified polycaprolactone, Polymer 39 (1998) 2883-2895.

[29] Q.X. Wu, N.A. Ma, T. Liu, E. Koranteng, Properties of compatible soy protein isolate/polycaprolactone composite with special interface structure, Polym. Composite. 40 (2019) E383-E391.

[30] T. Semba, K. Kitagawa, U.S. Ishiaku, H. Hamada, The effect of crosslinking on the mechanical properties of polylactic acid/polycaprolactone blends, J. Appl. Polym. Sci. 101 (2006) 1816-1825.

[31] H.J. Lee, H.K. Lee, E. Lim, Y.S. Song, Synergistic effect of lignin/polypropylene as a compatibilizer in multiphase eco-composites, Compos. Sci. Technol. 118 (2015) 193-197.

[32] M. Felix, I. Martinez, A. Romero, P. Partal, A. Guerrero, Effect of pH and nanoclay content on the morphology and physicochemical properties of soy protein/montmorillonite nanocomposite obtained by extrusion, Compos. Part. B-Eng. 140 (2018) 197-203.

[33] Q. Lv, D. Wu, H. Xie, S. Peng, Y. Chen, C. Xu, Crystallization of poly(ε-caprolactone) in its immiscible blend with polylactide: insight into the role of annealing histories, RSC Advances 6 (2016) 37721-37730.

[34] L. Chen, J. Jiang, L. Wei, X. Wang, G. Xue, D. Zhou, Confined Nucleation and Crystallization Kinetics in Lamellar Crystalline–Amorphous Diblock Copolymer Poly(ε-caprolactone)-b-poly(4-vinylpyridine), Macromolecules. 48 (2015) 1804-1812.

[35] Y. Yoneguchi, H. Kikuchi, S. Nakagawa, H. Marubayashi, T. Ishizone, S. Nojima, et al., Combined effects of confinement size and chain-end tethering on the crystallization of poly(ε-caprolactone) chains in nanolamellae, Polymer 160 (2019)

73-81.

[36] J.L. Kong, S.N. Yu, Fourier transform infrared spectroscopic analysis of protein secondary structures, Acta Bioch. Bioph. Sin. 39 (2007) 549-559.

[37] S. Krimm, J. Bandekar, Vibrational spectroscopy and conformation of peptides, polypeptides, and proteins, Advance in Protein Chemistry 38 (1986) 181-364.

[38] D.M. Byler, H. Susi, Examination of the secondary structure of proteins by deconvolved FTIR spectra, Biopolymers. 25 (1986) 469-487.

[39] S.D. He, J. Shi, E. Walid, H.W. Zhang, Y. Ma, S.J. Xue, Reverse micellar extraction of lectin from black turtle bean (Phaseolus vulgaris): Optimisation of extraction conditions by response surface methodology, Food Chem. 166 (2015) 93-100.

[40] M. Carbonaro, A. Nucara, Secondary structure of food proteins by Fourier transform spectroscopy in the mid-infrared region, Amino Acids 38 (2010) 679-690.

[41] H.-B. Yue, J.P. Fernandez-Blazquez, P.S. Shuttleworth, Y.-D. Cui, G. Ellis, Thermomechanical relaxation and different water states in cottonseed protein derived bioplastics, RSC Advances 4 (2014) 32320-32326.

[42] K. Murayama, M. Tomida, Heat-induced secondary structure and conformation change of bovine serum albumin investigated by Fourier transform infrared spectroscopy, Biochemistry. 43 (2004) 11526–11532.

[43] B.A. Khan, H. Na, V. Chevali, P. Warner, J. Zhu, H. Wang, Glycidyl methacrylate-compatibilized poly(lactic acid)/hemp hurd biocomposites: Processing, crystallization, and thermo-mechanical response, J. Mater. Sci. Technol. 34 (2018) 387-397.

[44] R.M. Silverstein, F.X. Webster, D.J. Kiemle. Spectrometric identification of organic compounds. 7th ed: John Wiley & Sons; 2006.

[45] N. Chandran, S. Chandran, H.J. Maria, S. Thomas, Compatibilizing action and localization of clay in a polypropylene/natural rubber (PP/NR) blend, RSC Advances 5

(2015) 86265-86273.

[46] B. Zhu, Y.M. Wang, H. Liu, J. Ying, C.T. Liu, C.Y. Shen, Effects of interface interaction and microphase dispersion on the mechanical properties of PCL/PLA/MMT nanocomposites visualized by nanomechanical mapping, Compos. Sci. Technol. 190 (2020) 108048.

[47] B.K. Wilson, R.K. Prud'homme, Processing Chitosan for Preparing Chitosan-Functionalized Nanoparticles by Polyelectrolyte Adsorption, Langmuir. 37 (2021) 8517-8524.

[48] N. Chandran, C. Sarathchandran, A. Sivadas, S. Thomas, Interfacial interaction in polypropylene-natural rubber blends: role of natural rubber on morphological, rheological, and mechanical evolution, J. Polym. Res. 29 (2022) https://doi.org/10.1007/s10965-10021-02873-10968.

[49] K. Dedecker, G. Groeninckx, T. Inoue, Reactive compatibilization of A/(B/C) polymer blends - Part 3. Quantitative analysis of the interfacial thickness and the interfacial reaction, Polymer 39 (1998) 5001-5010.

[50] J. Che, Y. Xiao, X. Wang, A. Pan, W. Yuan, X. Wu, Grafting polymerization of polyacetal onto nano-silica surface via bridging isocyanate, Surf. Coat. Tech. 201 (2007) 4578-4584.

[51] A.R. Ajitha, L.P. Mathew, Sabu Thomas, Chapter 6 - Compatibilization of polymer blends by micro and nanofillers, Compatibilization of Polymer Blends (2020) 179-203.

Figure captions

Fig. 1. SEM cross-section images of CP/PCL blend films (CP/PCL0, CP/PCL10, CP/PCL30, CP/PCL50, CP/PCL100). The bottom images are the enlarged areas marked with red boxes in the correspondent above images.

Fig. 2. (a) DSC heating and subsequent cooling curves of the CP/PCL blend biocomposites. (b) X-ray diffractograms of the biocomposites, with major diffraction peaks labelled.

Fig. 3. (a) FTIR spectra of the blend biocomposites. (b) The enlarged fitting curves of amide I and amide II bands estimating the percentage of protein secondary structure contribution (α-helix, β-sheet and β-turn).

Fig. 4. SEM cross-section images of the compatibilized samples (CP/PCL30/GMA1 and CP/PCL30/MA1) with the standard CP/PCL30 included for comparison.

Fig. 5. Demonstration of compatible reinforcement in CP/PCL blend biocomposites. (a) FTIR spectra of the biocomposites (CP/PCL30, CP/PCL30/GMA1 and CP/PCL30/MA1). The region where possible chemical reactions take place is enlarged in (b). (c) Tentative chemical reactions between functional groups of the compatibilizer and -OH or -NH_2 groups. (d) Schematic illustration of the compatibilizer-induced protein unfolding process.

Fig. 6. XPS spectra of the compatibilized sample (CP/PCL30/GMA1 and CP/PCL30/MA1) in comparison to the standard CP/PCL30. C1s spectra are shown in (a), (c), (e) and O1s in (b), (d), (f).

Highlights

- The reinforcement effects involving physically polymer chain interactions (e.g., transformation of protein secondary structure) and chemically reactive compatibilization provide new insights into the knowledge of compatibilization in terms of optimised interfaces within polymer blend biocomposites.
- The addition of small-molecule compatibilizer (e.g., glycidyl methacrylate) plays a critical role in increasing the protein/polycaprolactone interfacial bonding and co-continuous phase formation, further enhancing mecahnical, themal, and hydrophobic properties of the biocomposites.
- Mechanial and thermal properties of the biocomposites can be significantly improved by simply tuning the content of reinforcing polycaprolactone.
- Cottonseed protein/polycaprolactone blend biocomposites can be easily fabricated by melt-compounding and hot pressing.